AGILE: GIScience Series, 7, 2, 2026. https://doi.org/10.5194/agile-giss-7-2-2026
Proceedings of the 29th AGILE Conference on Geographic Information Science, 16–19 June 2026.
Eds.: Evelyn Uuemaa, Alexander Kmoch, Holger Virro, and Simon Scheider
This contribution underwent peer review based on a full paper submission.

A Method for Spatializing Disturbance by Detecting Human-Wildlife Encounters from GNSS Trajectories

John Dawson [1,2], Veronika Peralta [2], Ana-Maria Olteanu-Raimond [1], Thomas Devogele [2], and Mathieu Garel [3]

[1]LASTIG, Univ Gustave Eiffel, IGN-GéoData Paris, Paris, France
[2]LIFAT, University of Tours, Blois, France
[3]Office Français de la Bodiversité, Gières, France

Correspondence: John Dawson (John-Andrew.Dawson@IGN.fr)

Abstract.

A significant source of human pressure on the environment originates from human-wildlife encounters during recreational activities in natural spaces. These events are difficult to study given their short duration, as well as the sparsity and granularity of concurrently tracked human and wildlife data.

Wildlife often perceives and reacts to human presence over distances greater than GNSS uncertainty. Thus, we propose a new encounter detection method that incorporates a broader range of human disturbance as opposed to addressing incompleteness, enabling us to identify where and when human-wildlife encounters are most likely to occur, and thus offering a more ecologically realistic assessment of encounter risk.

The method was applied on a pilot study in the Bauges massif in the French Alps, leveraging semantically enhanced chamois and human trajectories. A spatio-temporal analysis of human-wildlife encounter results is presented to demonstrate how the method can support ecologists or stakeholders in gaining deeper understanding of wildlife behavior or in taking actions to mitigate human impacts.

Submission Type. Algorithm, Case Study.

BoK Concepts. [CF5-6] Spatial distribution, [GS4-3b] Citizens and volunteered geographic information, [AM8] Geostatistics.

Keywords. human-wildlife encounters, pressure zones, semantic trajectory enhancement, human-wildlife GPS tracking.

1 Introduction

Studying spatio-temporal interactions between mobile objects is complex and fundamental to many fields of research: accidentology (Huang et al., 2020), criminal investigations (Daubal et al., 2013), crowded surveillance (Boukhers et al., 2016), and ethology (Lührs and Kappeler, 2013). Particularly interactions between vehicles, animals, or humans are challenging to study due to heterogeneous data sources, varying spatial–temporal resolutions and missing information. This article uses human-induced disturbances in animal activity as a case study to address general issues of mobile-object interactions with heterogeneous data quality.

In recent years, the use of natural spaces for recreation has increased globally (Balmford et al., 2015). Overuse of trails can physically degrade the trails and change the bordering flora (Ólafsdóttir and Runnström, 2013; Marion et al., 2006); these progress temporally but are continually visible unlike the increased pressure on wildlife.

Encounters with people exert multiple pressures on wildlife, including increased stress levels (Stankowich, 2008), increased time spent in an alert state or fleeing, and reduced time available for essential tasks, such as foraging (Taylor and Knight, 2003). Furthermore, repeated encounters can lead wildlife to abandon high value areas to avoid humans (Courbin et al., 2022). Understanding the effects of human presence is complicated by species-specific sensitivities to human behavior (Stankowich, 2008; Taylor and Knight, 2003).

This paper deals with detecting and quantifying human-wildlife encounters with the hypothesis that they may reveal meaningful patterns that increase understanding of human-wildlife interaction and support ecosystem monitoring and decision-making.

Quantifying the timing, frequency and locations of human-wildlife encounters is challenging. First, surveys of natural-area users are imprecise and incomplete, as participants vary in awareness of their effects on wildlife and often fail to notice or record visible animals (Long, 2019). As such, direct observation from participants cannot be taken as an exhaustive ground truth. Second, detecting human-wildlife encounters from global navigation satellite system (GNSS) recorded data suffers from imprecision due to varying sampling rates for both humans and animals. In particular, wildlife recorded data has significant variations in sample rate caused by the limits in the technology and the difficulty of tagging animals. Finally, seasonal and diurnal variations in space usage of humans and animals result in temporal fluctuations in pressure distribution.

This paper proposes an encounter detection method that estimates human disturbance areas to determine where and when encounters occur most frequently. The contributions are: (i) a disturbance-based definition of encounters, (ii) a novel encounter detection method, and (iii) a case study illustrating many typical user analysis tasks.

The paper is organized as follows: Section 2 discusses related works, Section 3 describes our methodology, Section 4 details experimental setup; Section 5 presents the results and Section 6 concludes and discusses future works.

2 Related Work

This section discusses related work on human-wildlife encounter detection methods for GNSS trajectories.

Various definitions exist to characterize spatio-temporal relationships between moving objects. For animal data, Doncaster (1990) defined a static interaction as the overlapping space use over a period of time such as having overlapping home ranges. A dynamic interaction is defined as an event where two moving objects are closer than a distance threshold at the same time (Miller, 2015; Dodge et al., 2021). The ORTEGA package (Su et al., 2024), expanded these definitions by distinguishing encounters (brief events) from interactions (longer events implying mutual influence).

Concerning methods for detecting encounters, most focus on accounting for the uncertainty in position between GNSS points and search for overlapping space usage. Thus, a major challenge is inconsistent or poor data with spatio-temporal granularity. Proximity-based methods that use spatio-temporal thresholds around a GNSS point are sensitive to threshold choices and data granularity (Dodge et al., 2021). In particular, crossing trajectories that are sampled sparsely in time could be missed. Several methods use space-time prisms (STP) (Spaccapietra et al., 2008) to estimate the possible locations of a tracked object in-between known positions. These methods combine the object's maximum speed and the elapsed time between consecutive points to determine its possible locations.

Many methods have been proposed using either vector or raster geometry. Long et al. (2015) applied a vector-geometry approach using two-denominational STP called potential path areas (PPA) to find encounters by searching for overlapping PPA at the same time t_τ. ORTEGA is an open source Python library to detect and analyze encounters using PPAs spanning the entire duration between consecutive points. The ORTEGA method has been applied to both human-human and animal-animal encounters (Su et al., 2024; Dodge et al., 2021).

The raster approach of Downs et al. (2014) selects all cells meeting STP requirements for each time step t_τ between GNSS points. Each cell is assigned a probability, at t_τ, using inverse-distance weighting from the expected position along a line connecting the points; encounters are then detected by overlapping the resulting probability maps. Encounter probability is calculated from overlapping cell probabilities; the method was demonstrated on intra-zebra encounters with a small dataset. Furthermore, Ho and Loraamm (2023) replaced inverse-distance weighting with a cost-distance method based on the animals land-use preferences, determining the probability of an animal being in a given cell at a particular time.

Moreover, Yin et al. (2019) extended this method by introducing an intervisibility check, using a digital elevation map to determine whether terrain obstructs the line of sight between two points.

The above methods focus on encounters between similar moving objects and lack methods to estimate the distance at which they influence each other. We claim that intersecting $PPAs$ alone cannot capture human disturbance to wildlife, especially when human data is well-sampled (thus $PPAs$ are thin) and when the area of influence is broad.

Another challenge in trajectory analysis is dealing with large amounts of high sample rates trajectories, which necessitates simplification methods without compromising the overall shape of the movement. The Douglas-Peucker algorithm simplifies trajectories by recursively removing points that do not alter their overall shape, enabling faster processing (Douglas and Peucker, 1973; Ramer, 1972).

To the best of our knowledge, there is no human-wildlife encounter detection method estimating the area of human disruption. In this paper, we propose a new optimized method to identify encounters between numerous highly-sampled trajectories of dissimilar moving objects, accounting for significant disturbance distances.

3 Proposed Methodology

This section introduces key concepts (Table 1) and describes the proposed encounter detection method.

3.1 Core Concepts

Following CONSTAnT model (Bogorny et al., 2014), a trajectory $\mathcal{T} =< P_1 ... P_N >$ is an ordered list of GNSS points with position and timestamp that record a moving object's location at specific times. A GNSS point is represented as $P_k = (p_k, t_k)$ where p_k is a position and t_k a timestamp.

Hereafter, the superscript h with index i denotes human points ($P_i^h = (p_i, t_i)$), superscript a and index j indicate animal points ($P_j^a = (p_j, t_j)$), while index k represents generic points, related to both.

Table 1. Concept Acronyms

Concept	Acronym
Human point	$P_i^h = (p_i, t_i)$
Animal point	$P_j^a = (p_j, t_j)$
Point position	$P_k(p)$
Point timestamp	$P_k(t)$
Human disturbance area	$HDA_{i,i+1}$
Potential path area	$PPA_{j,j+1}$
Available area	AA_m
Encounter event	EE_k
Encounter event initial time	$EE(t_0)$
Encounter event final time	$EE(t_f)$
Day of year	doy
Obstacles preventing disturbance	Ω
Encounter	EC
Encounter duration	$EC(\Delta t)$
Encounter area^{animal}	ECA^a
Encounter area^{human}	ECA^h

Two indicators assess trajectory completeness: *Temporal granularity*, the number of recorded points divided by trajectory duration, and *Spatial granularity*, the number of points divided by trajectory length. Higher values indicate greater granularity.

As animal trajectories often have low spatio-temporal granularity, we utilize PPA to address incompleteness, as in previews works (Su et al., 2024; Dodge et al., 2021; Downs et al., 2014). The human trajectories have much higher granularity, producing PPAs substantially smaller than typical wildlife disturbance distances. Thus, directly intersecting PPAs, as done by related works, often misses encounters. We define a new concept, human disturbance area (HDA), to represent the wide area of human influence on wildlife.

3.1.1 Human Disturbance Area (HDA)

A HDA represents the area where human activity has an effect on wildlife and is estimated from a human trajectory.

Definition 1. *Thus, given two consecutive GNSS points in a human's trajectory, P_i^h and P_{i+1}^h, and a distance threshold, expressed as HDA_radius, $HDA_{i,i+1}$ is computed as a buffer of radius HDA_radius around the line segment $[P_i^h(p), P_{i+1}^h(p)]$.* □

Figure 1 illustrates the HDA (colored area) for two points in a human trajectory. As animals react differently to intrusion, the distance threshold HDA_radius should be set considering contextual factors including the activity being performed by both the human and animal, the alert distance of the animal, and environmental conditions.

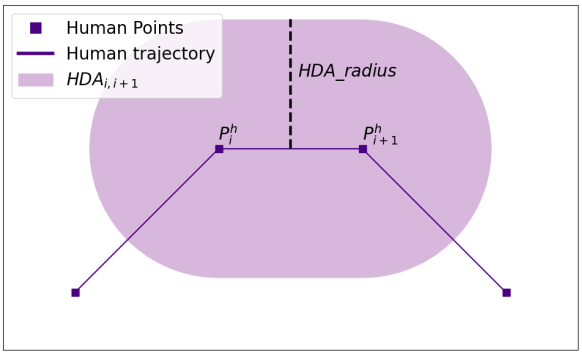

Figure 1. Example of HDA, with radius HDA_radius.

3.1.2 Potential Path Area (PPA)

A PPA is the entire area a recorded animal could have occupied in-between two GNSS points P_j^a and P_{j+1}^a. It is computed as in the ORTEGA package using the maximum speed of the animal and the amount of time elapsed between the points $[P_j^a(t), P_{j+1}^a(t)]$ (Su et al., 2024; Dodge et al., 2021; Long et al., 2015).

Definition 2. *Thus, given two GNSS points P_j^a and P_{j+1}^a, a PPA is computed as $PPA_{j,j+1} = \cup_{m \in [j,j+1]} AA_m$, where AA_m is the entire area that the animal could have been at any in-between time $t_m \in [P_j^a(t), P_{j+1}^a(t)]$ while still being able to be at both positions P_j^a and P_{j+1}^a without exceeding the maximum speed the animal can achieve (v_{max}).*

AA_m is computed as the intersection of two circles, respectively centered at $P_j^a(p)$ and $P_{j+1}^a(p)$, having as radius $v_{max} \cdot (t_m - P_j^a(t))$ and $v_{max} \cdot (P_{j+1}^a(t) - t_m)$. These radiuses represent the distance the animal could have traveled in the elapsed time away from $P_j^a(p)$ and the distance the animal can be away from $P_{j+1}^a(p)$ and still be able to reach it in the remaining time respectively. □

Figure 2 illustrates the computation of a PPA. Circles represent the possible distance the animal could be away from $\boldsymbol{P_j^a}$ and $\boldsymbol{P_{j+1}^a}$ at $\boldsymbol{t_m}$, with the darker area (at the intersection of the two circles, representing the AA_m at time t_m). The union of these AA_m, obtained by varying m, results in the lighted-colored area, which defines the PPA.

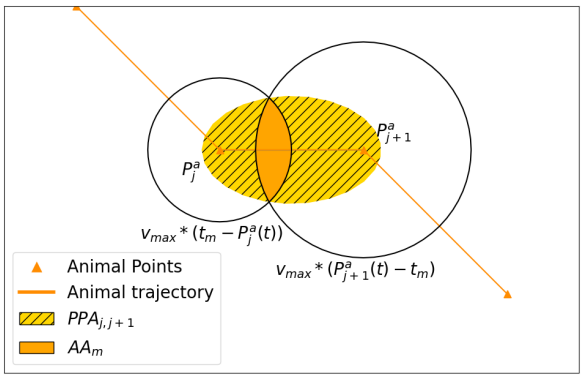

Figure 2. Example of a potential path area $\boldsymbol{PPA}$, where $\boldsymbol{AA_m}$ represents the available area the animal could have occupied at time $\boldsymbol{t_m}$.

3.2 Encounter Concepts

We define encounters between human and animal trajectories as areas where humans are close enough in space and time to likely disturb animals.

We use HDA and PPA to define spatial overlapping, also considering the presence of obstacles preventing disturbance. Temporal intersection is defined by the same time of the day and a close date. We do not impose date overlapping, to be more representative of actual trajectories and consider potential encounters. As recorded trajectories represent only a fraction of actual trajectories, unrecorded trajectories likely use space similarly (e.g. animals have recurrent spatial behavior, humans follow paths). A threshold defines acceptable distance in date. Encounters on the same date are called $real$, while those on different dates $potential$.

3.2.1 Encounter Event (EE)

An EE is a spatio-temporal co-occurrence where a human likely disturbed an animal.

Definition 3. *Thus, EE is defined as a pair of consecutive human points and linked to a pair of consecutive animal points $EE_k = (P^h_i, P^h_{i+1}, P^a_j, P^a_{j+1})$ that satisfy the following conditions:*

1. *a human came close enough spatially to disrupt the animal behavior, i.e., $HDA_{i,i+1} \cap PPA_{j,j+1} \neq \emptyset$.*
2. *there is temporal intersection between them, i.e.,*

$$[time(P^h_i), time(P^h_{i+1})] \cap [time(P^a_j), time(P^a_{j+1})] \neq \emptyset.$$

3. *trajectories took place on close dates, i.e.,*

$$|doy(P^h_i) - doy(P^a_j)| \leq doy\_shift.$$

4. *no obstacle is preventing the human from disturbing the animal, i.e., $\Omega(HDA_{i,i+1}, PPA_{j,j+1}) = \emptyset$*

where Ω indicates a set of obstacles between a PPA and a HDA, $doy(P^h_i)$ represents the day of year (the number of days from January 1st) of a point, and $time(P^h_i)$ represents the time of the point (without the date component). □

Criteria preventing EEs are context-specific and may include various obstacle types. For example, for an animal that detects threats using vision, an obstacle could be something blocking visibility. Other obstacles, such as rivers or gullies, could prevent animals from feeling threatened by humans.

The threshold doy_shift defines a cut off for how far apart in day of year unrecorded trajectories are likely to show similar behavior to recorded trajectories. For example, if an animal was recorded on April 1st and a human passed the same area at the same hour on April 2nd, it is reasonable to think an untracked animal was present on April 2nd.

$EE(t_0)$ and $EE(t_f)$ denotes the times of the initial $(P^h_i(t))$ and final $(P^h_{i+1}(t))$ human points, in an EE. These EE are formalized and depicted as a bipartite graph as depicted in Figure 3.

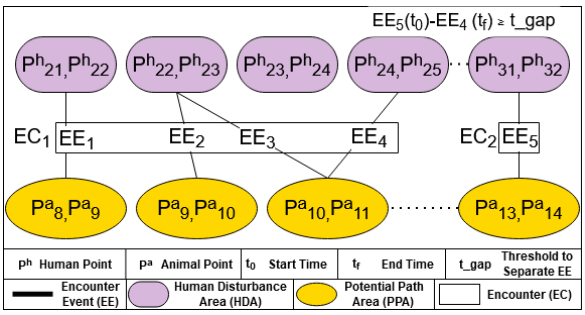

Figure 3. Example of the components of two encounters, the relationship between points ($\boldsymbol{P}$), $\boldsymbol{EE}$, $\boldsymbol{PPA}$ and $\boldsymbol{DA}$.

3.2.2 Encounter (EC)

An encounter is defined as the spatio-temporal instance where human presence may have affected an animal's behavior and consists of a temporally-close set of EE between a human and animal trajectories.

Definition 4. *Thus, EC is defined as a series of encounter events between two trajectories $EC =< EE_1, ...EE_n >$ where $EE_{k+1}(t_0) - EE_k(t_f) < t\_gap$, for $1 \leq k \leq n-1$.* □

The t_gap threshold separates encounters when the animal has time to return to an unalert state between EEs, and should be set based on the desired granularity of encounters. Without this parameter, outbound and return encounters could merge into one misleadingly long encounter.

Consistent with previous notations, we use $EC(\Delta t)$ to refer to the duration of the encounter (computed from initial and last human points).

Figure 3 illustrates how the previous concepts are related to one another. We observe that an HDA or a PPA can be linked to multiple counterparts, and that some $HDAs$ or $PPAs$ may be excluded due to some unmet spatial or obstacle conditions. Finally, when encounter events are separated in time, they are considered in separated encounters (e.g., EC_2).

An encounter has two geometries: Encounter Area^{animal} (ECA^a) and Encounter Area^{human} (ECA^h) defined below.

3.2.3 Encounter Area^{animal} (ECA^a)

ECA^a is the area an animal may have occupied when it was involved in an encounter.

Definition 5. *Thus, given an encounter* $EC =< EE_1, ...EE_n >$, ECA^a *is the union of* PPA *of the encounter events,* $ECA^a = \cup_{k=1}^{n} PPA^k$, *where* PPA^k *is the* PPA *of the animals points in* EE_k. □

An example of ECA^a can be seen in Figure 4.

3.2.4 Encounter Area^{human} (ECA^h)

Similarly, ECA^h represents the area occupied by humans during the encounter i.e., the source of disturbance. ECA^h is computed around the same line segments as the $HDAs$ of the human points involved in the encounter but with a smaller buffer.

Definition 6. *Thus, given an encounter* $EC =< EE_1, ...EE_n >$, $ECA^a = \bigcup_{k=1}^{n} resize(HDA^k, ECA^h\_radius)$, *where* HDA^k *is the* HDA *of the human points in* EE_k, *and* $resize$ *is a function that creates a new buffer around the* HDA *line segment with a radius of* ECA^h_radius. □

An example of the ECA^h can be seen in Figure 4. The radius of this buffer should be based on the uncertainty in human position.

3.3 Encounter Detection Method

The encounter detection method below utilizes a number of elements from earlier works including Douglas-Peucker filtering (Meratnia and de By, 2004), potential path areas (Long et al., 2015), and intervisibility detection (Lonergan and Hedley, 2016). This method contributes novel formalizations for potential encounters, HDA_{radius}, and EE; and a novel combination of PPA, HDA_{radius} and obstacle criteria in the form of intervisibility. Both real and potential encounters are detected and are distinguished in Step 2.

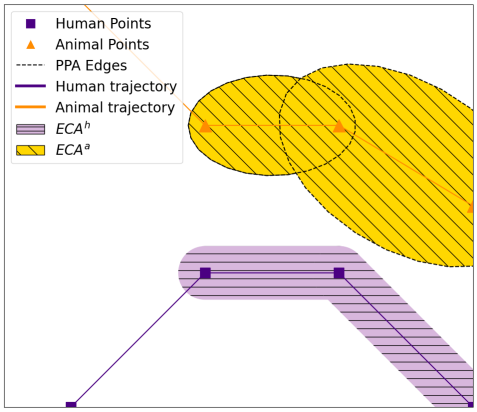

Figure 4. Example of a paired ECA^h, and ECA^a composed of two encounter events.

The method's workflow is summarized below and illustrated in Figure 5.

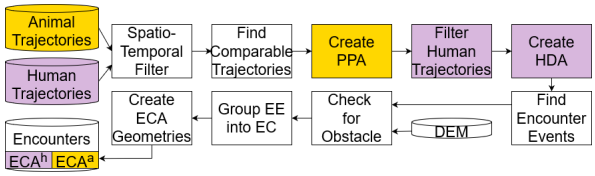

Figure 5. Workflow of the encounter detection method, with human-related steps in purple and animal-related ones in yellow. Cylinders indicate input or output data, and DEM is digital elevation model.

1. **Spatio-Temporal Filter:** Remove outliers and trajectories with insufficient temporal granularity.
2. **Find Comparable Trajectories:** Human and animal trajectories with overlapping time of day and close day of year (less than $\boldsymbol{doy\_shift}$) are selected.
3. **Create $\boldsymbol{PPA}$:** Generate $PPAs$ for consecutive animal points (Def. 2) using the animal's $\boldsymbol{max\_speed}$.
4. **Filter Human Trajectories:** Apply spatial filtering and temporal resampling to simplify trajectories while preserving key spatio-temporal characteristics. Human trajectories are filtered using Douglas-Peucker method with a distance threshold $\boldsymbol{min\_dist}$ then points are re-added from the unfiltered trajectory to maintain a sample frequency of $\boldsymbol{min\_time}$ when possible.
5. **Create $\boldsymbol{HDA}$:** Create $HDAs$ (to Def. 1), as buffers of size $\boldsymbol{HDA\_radius}$ around line segments between consecutive points. $HDAs$ with endpoints farther apart than a distance threshold $\boldsymbol{d\_gap^h}$ are discarded as it indicates a gap in recorded data.
6. **Find Encounter Events:** Create EE for spatially and temporally overlapping $PPAs$ and $HDAs$ (criteria 1 and 2 in Def. 3).

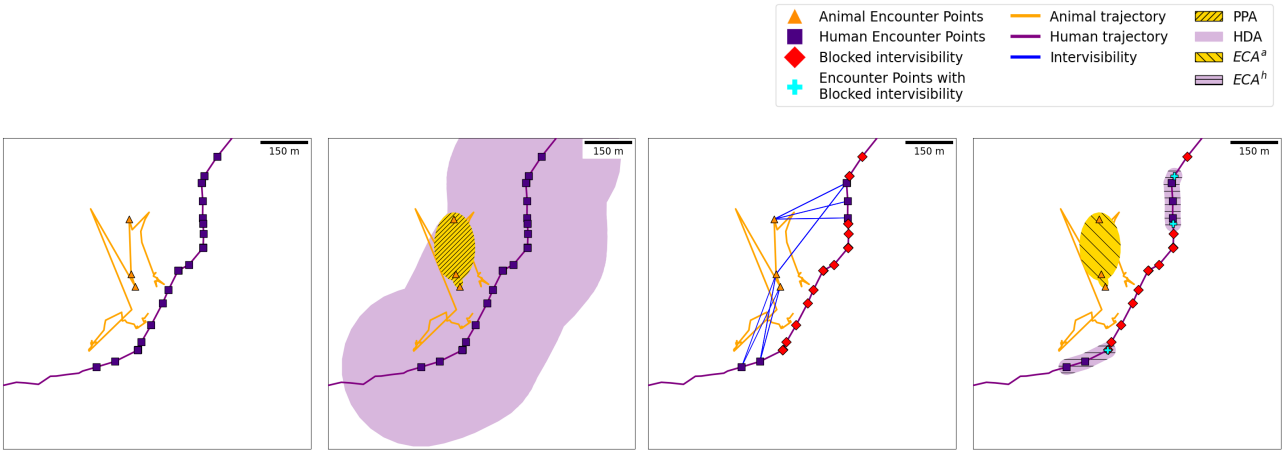

(a) Steps 1-2 (b) Steps 3-6 (c) Step 7 (d) Steps 8-9

Figure 6. Depiction of major steps of encounter detection method for an example encounter. Encounter points without intervisibility that are part of a PPA or HDA in which the other point has visibility are included in encounters.

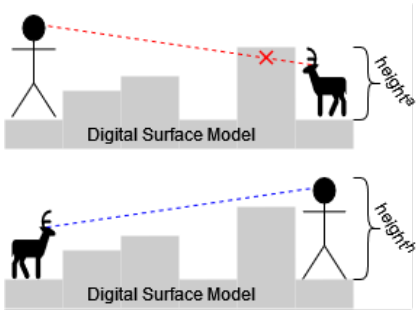

Figure 7. Depiction of intervisibility calculation using line-of-sight analysis (i.e., mutual visibility.)

7. **Check for Obstacle:** Check obstacle conditions to filter out any invalid EEs. In this paper, intervisibility is implemented to check for terrain, which requires heights for animals and humans, $\boldsymbol{height^a}$ and $\boldsymbol{height^h}$ respectively, and a digital elevation model, DEM. Figure 7 depicts an example of this calculation.

8. **Group $\boldsymbol{EE}$ into $\boldsymbol{EC}$:** EE closer than a time threshold $\boldsymbol{t\_gap}$ are grouped into an EC as in Def. 4.

9. **Create $\boldsymbol{ECA}$ geometries:** For each encounter, ECA^a and ECA^h are created following Def. 5 and Def 6, with threshold $\boldsymbol{ECA^h\_radius}$.

Figure 6 illustrates the detection of an encounter between two trajectories. (a) shows the original trajectories with the points involved in the encounter. (b) displays the corresponding PPAs and HDAs (only geometries in the encounter). (c) presents the intervisibility check, and (d) the resulting ECA^a and ECA^h. Note that ECA^h has two sections due to a loss of intervisibility, but since the blocked intervisibility duration is shorter than t_gap, they are considered part of the same encounter.

3.3.1 Data and Software Availability

The code used to create results, tables and figures included in this paper are available at the github link https://github.com/IntForOut/Human_Wildlife_Encounter_Detection.

Due to privacy concerns with human GPS data, we cannot publicly publish the entire dataset. But a restricted access repository containing the dataset was made available for reproducibility review.

The method is primarily written in Python with database management and some encounter detection steps performed in PostgreSQL/PostGIS, with intervisibility analysis using the QGIS Visibility Analysis plugin (Čučković, 2025), the Tracklib Library for trajectory management (Méneroux and van Damme, 2024) and modified sections of the ORTEGA package (Su et al., 2024). Road network data is from BD Topo database (IGN, 2025) and the digital elevation map is from 25m resolution BD Alti (IGN, 2025). The chamois dataset is hosted on Movebank, with the id: "3336284355".

3.3.2 Generalization

This framework is generalizable and can be adapted to other species and contexts by adjusting the HDA_radius, modifying or removing the doy_shift, and selecting obstacles that reflect the site fidelity and behavior of the target species. For example, when applying this method to species that depend on hearing for threat detection (e.g. red deer in dense forests), the HDA_radius could be reduced and the visibility constraint removed. For species exhibiting strong site fidelity (e.g., remaining close to a den or refuge), the doy_shift can be retained.

In contrast, adapting the method for wide-ranging opportunistic predators (e.g. wolves) may require increasing the HDA_radius to reflect their high

responsiveness to human presence and extending it in the prevailing wind direction to account for scent-based threat detection. Given their large territories and ability to navigate anthropized landscapes, the doy_shift should be reduced or limited to real encounters only.

4 Experiments

This section describes the implementation of the encounter detection method and its instantiation on human and chamois trajectories recorded in the French Alps.

4.1 Study Area

Our study was conducted in the National Game and Wildlife Reserve of the Bauges Massif, located in the French Alps (Figure 8; 45°40'N, 6°13'E). This predominantly mountainous region ranges in elevation from 900 to 2200 meters and features a landscape largely covered by forests (56%), with the treeline situated around 1500 meters. The remainder is composed primarily of grasslands and some rocky outcrops. The reserve attracts a high number of visitors annually (over 37,000 individuals, primarily during the summer), with 1.1 million overnight stays recorded in summer and 0.5 million in winter in 2014 (Thel et al., 2024). Nearly all hiker activity is concentrated on a network of marked trails across alpine grasslands, resulting in spatially concentrated human disturbance to wildlife (Courbin et al. 2022; Figure 8). Chamois in the area face limited natural predation, with occasional threats to young or injured individuals. Regulated hunting occurs within the reserve, from early September to late February, carried out by small parties (3–4 hunters), primarily targeting chamois, which is the main ungulate species living in the Wildlife Reserve (Courbin et al., 2022).

4.2 Data

In this work, we use chamois (*Rupicapra rupicapra rupicapra*) data from a long-term Capture-Mark-Recapture program, and human trajectories from crowdsourced platforms and a survey project (Kerouanton, 2020). Chamois form stable socio-spatial clusters, with several individuals sharing the same limited and accessible ranges. These groups show strong site fidelity, repeatedly using the similar areas seasonally and yearly (Darmon et al., 2012; Duparc et al., 2019). They also primarily use vision to detect threats (Hamr, 1988).

This dataset contains 82,685 trajectories for 257 recorded animals (218 females and 39 males), where each trajectory represents a single day's record. Note that the animals were trapped in specific areas (4 trapping sites; Figure 8) to which they are strongly attached and thus, they do not represent the full population distribution.

The chamois sampling frequency varies significantly, from a single point a day to a point every ten minutes (Table 2).

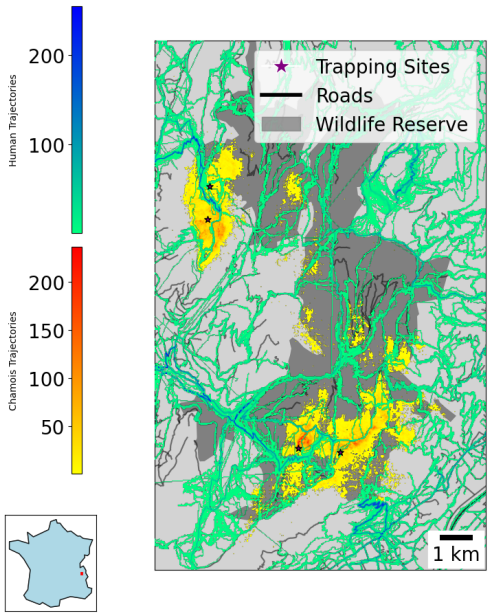

Figure 8. GNSS trajectory density for humans and chamois in the Bauges massif, and chamois trapping locations.

Only 22% of the trajectories with a sample frequency of at least one point per hour were used for encounter detection. For now, low-frequency trajectories were excluded to limit uncertainty, as they require additional analysis to determine their effects on the results. This data will be analyzed in future works.

The majority of the human GNSS data were crowdsourced via APIs from the websites listed in Table 3, where people have shared their GNSS registered data during outdoor activities (e.g. hiking, running), and a second part is from a survey project (Kerouanton, 2020); human data was anonymized with new random IDs. The survey data was from groups of hikers who were given a single GNSS receiver at trail entrances; all participants were given surveys when returning the GNSS receiver (Kerouanton, 2020). These data sources differ in accuracy and sampling frequency. As illustrated by the averaged values in Table 3, the human data have substantially higher temporal granularity than chamois data, but similar spatial granularity. On most days, the chamois move very little resulting in good spatial granularity with few points. Because human and chamois have trajectories that leave the reserve, analysis was not constrained to its boarders.

Table 2. Chamois data sampling (* unused trajectories)

Number of trajectories	Temporal granularity (point/min)	Spatial granularity (point/meter)
121	$\leq$ 1/10	1/29
4,035	[1/10-1/20]	1/51
2,603	[1/20-1/30]	1/110
12,414	[1/30-1/60]	1/72
63,573*	$>$ 1/60	—

Table 3. Human data by sources

Source	Number of trajectories	Temporal granularity (points/sec)	Spatial granularity (points/m)
CampToCamp	10	1/60	1/39
GPSRando	6	1/13	1/8
Strava	2282	1/1	1/3
Visu	211	1/3	1/5
VTTour	44	1/5	1/11
Survey project	281	1/4	1/5

Table 4. Parameter Settings

Name	Step	Value
doy_shift	2 : Find Comp Traj	15 days
max_speed	3 : Create PPA	1.25*spd
d_gap^a	3 : Create PPA	500 m
min_dist	4 : Filter Human Traj	25 m
min_time	4 : Filter Human Traj	1 min
HDA_radius	5 : Create HDA Traj	250 m
d_gap^h	5 : Create HDA Traj	500 m
$height^h$	7 : Check for Obstacle	1.6 m
$height^a$	7 : Check for Obstacle	1 m
t_gap	8 : Group EE into EC	8 min
ECA^h_radius	9 : Create ECA geom	10 m

4.3 Preprocessing

The data was preprocessed differently depending on the type of recorded moving object. Outlier filtering was first applied: chamois trajectories followed Bjørneraas et al. (2010), and human trajectories followed Ivanovic (2018), both using geometric and temporal indicators from GNSS points.

Second, temporal filtering excluded 25 trajectories lacking timestamps; missing timestamps in other trajectories were linearly interpolated.

Thirdly, spatial filtering is applied with the Douglas–Peucker algorithm, after which original points were reinserted where time gaps exceeded a threshold min_time to preserve temporal granularity. This choice was preferred over simple resampling as Douglas-Peucker will find points that are important to the trajectories shape even if they are closer in time than the resampling rate.

4.4 Settings

Encounter detection was conducted using the following parameters, listed in Table 4 with their corresponding steps.

A 250 meter HDA_radius was selected to be slightly higher than the average distance that chamois move away from the trails during the day (190 meters) (Courbin et al., 2022). This distance is likely a safety distance that chamois maintain from the trail during the day to avoid people, and could indicate the distance at which a human approaching starts to disturb them. HDA size influences the included points, the duration, the shape, and the total number of encounters.

PPA geometry followed ORTEGA defaults (Su et al., 2024), with maximum speed as 1.25 × speed observed between points.

Doy_shift was set to 15 days to take into account the limited representativeness of both animals and human data (e.g. only recorded animals and only connected practitioners sharing their data). This large Doy_shift value was selected because chamois often remain in the same area for consecutive days, meaning that individuals recorded on one day were likely still present on unrecorded days (Crampe et al., 2007). Since it only determines trajectory pairings without affecting the encounters, encounters can be filtered by doy_shift without rerunning the detection.

T_gap was set to 8 minutes. This parameter separates repeated encounters between trajectory pairs.

Thresholds d_gap^a and d_gap^h were both 500 m, removing segments with insufficient spatial granularity to prevent over-detection.

Filtering used min_dist = 25 m and min_time = 1 min maintain temporal granularity and trajectory shape while decreasing runtime.

Intervisibility analysis assumed $height^h$ = 1.6 m and $height^a$ = 1 m.

Seasons are defined as spring (March - May), summer (June - August), fall (September - November), and winter (December - February). These ranges ensure equal seasonal duration and year-round coverage. Fall was set to match the peak hunting period and the rutting period in males (Courbin et al., 2022), while the start of summer was set as the mean chamois birth date. The winter-spring transition marks hunting closure, and maintains equal length seasons.

5 Results

This section presents the general statistics of the detected encounters, followed by analytical approaches that illustrate how encounters can be used and interpreted.

5.1 Overall Encounter Analysis

Applying the encounter detection parameters from Section 4.4 resulted in 63,263 encounters (of which 185 were $real$ encounters). The large discrepancy between real and potential encounters is primarily due to the broader matching window. Real encounters are restricted to the same day, whereas potential encounters allow a ± 15 difference in day-of-year, resulting in substantially

more trajectory comparisons (15,083 vs. 4,500,532). The location of all ECA^a and ECA^h are depicted in Figure 9. The low number of real encounters likely reflects limited trajectory data and chamois proactively avoiding humans (Courbin et al., 2022).

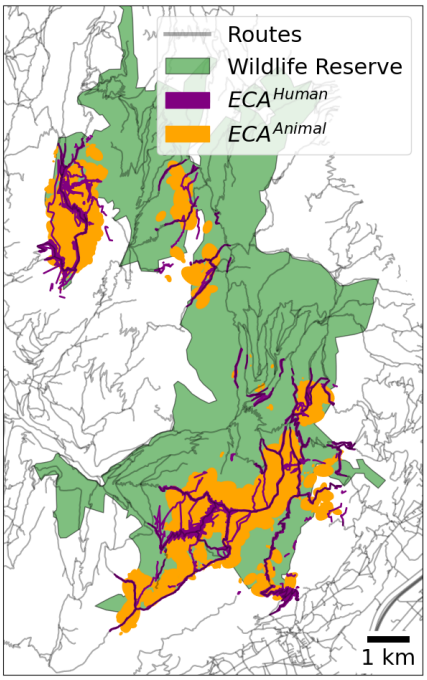

Figure 9. Depiction of all $\boldsymbol{ECA^h}$ and $\boldsymbol{ECA^a}$ detected in this data set.

The northern and the southern clusters of ECA^a seen in Figure 9 align with the home ranges of the tagged animals described in Courbin et al. (2022).

Because chamois often stay in one area for days, repeated encounters occur between distinct human trajectories and multiple trajectories from the same chamois. Thus, humans following the same route on the other days would have disturbed the animal. This provides justification for the use of potential encounters, as they suggest that chamois may remain in a location when their GNSS tag is not actively recording. Nevertheless, repeated potential encounters between the same individuals must be addressed when analyzing the results to avoid bias.

5.1.1 Intervisibility

Enforcing intervisibility affected the number of encounters detected, the size of ECA^h and ECA^a, and the duration of encounters, as fewer EE were valid. Intervisibility reduced EE by 58.3 % while ECs are only 15.6 % lower than when not requiring intervisibility. This is caused by the removal of EEs from ECs; its effects are shown in Table 5.

EEs between more distant human–animal trajectories are more affected by intervisibility, causing fewer ECs at greater distances; this can be seen in Figure 10. Thus,

Table 5. Effects of $\boldsymbol{HDA\_radius}$ and Intervisibility on Encounter Metrics

Metric	Default	HDA_radius = 500 m	Intervisibility Ignored
EE [count]	663,357	1,735,923	1,592,066
EC [count]	63,263	108,958	74,978
$EC(\Delta t)[min]$	12:02	17:45	21:21
ECA^h [m^2]	6,413	9,089	10,165
ECA^a [m^2]	12,079	11,403	13,017

intervisibility grows in importance as HDA_radius increases. For instance, when HDA_radius is 500 m, intervisibility removes 70.1 % of EEs, and 20.8 % of ECs.

5.2 Sensitivity Analysis

This section discusses the effects of parameters listed in Table 4. Due to the lack of a ground truth for validation, the impact of varying each parameter will be examined to determine the most critical parameters and understand the robustness of the model. In the following discussion, all parameters will match those in Table 4, except for the one being analyzed. The effects of changing a parameter on the total number of EEs and encounters is presented in Table 6. The results presented below are ordered by a priori importance of the parameters.

500 m was used as a second HDA_radius, as it represents the maximum distance at which chamois respond to humans representing a realistic upper limit (Hamr, 1988). Larger HDA_radius increase the number of PPAs and HDAs intersections. This increased the number of EE resulting in more encounters with larger

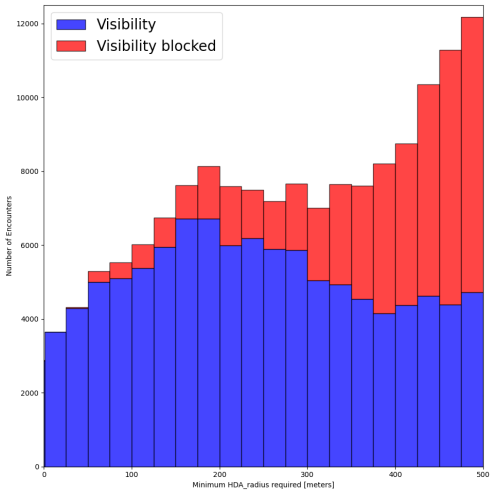

Figure 10. Histogram of encounters, where the x-axis shows the minimum value of HDA_radius required to detect each EC. Blocked intervisibility refers to instances that would be classified as EC if intervisibility was not required. This histogram is not cumulative between bins.

Table 6. Effect of Parameters on $\boldsymbol{EE}$ and $\boldsymbol{EC}$ Detection

Parameter	Value	No. EE	No. EC
–	Default	**663,357**	**63,263**
doy_shift	0	21,844 (-96.7 %)	2,053 (-96.8 %)
doy_shift	1	63,197 (-90.5 %)	6,015 (-90.5 %)
doy_shift	2	106,716 (-83.9 %)	10,191 (- 83.9%)
doy_shift	3	149,371 (-77.5%)	14,342 (-77.3 %)
doy_shift	14	620,183 (-6.5 %)	59,099 (-6.6 %)
d_gap^a	None	683,116 (+3.0 %)	64,510 (+2.0 %)
d_gap^h	None	663,935 (+0.1 %)	63,423 (+0.2 %
HDA_{radius}	500 m	1,735,923 (+161.7 %)	108,958 (+72.2 %)
$height^h$	2 m	Same (+0.0 %)	Same (+0 %)
$height^a$	0.8 m	648,880 (-2.2 %)	62,834 (-0.7 %)
$height^a$	1.2 m	675,810 (+1.9 %)	63,759 (+0.8 %)
t_gap	2 min	Same (+0.0 %)	81,413 (+28.7 %)
t_gap	4 min	Same (+0.0 %)	70,881 (+12.0 %)
t_gap	16 min	Same (+0.0 %)	58,020 (-8.3 %)
t_gap	2 hour	Same (+0.0 %)	50,792 (-19.7 %)
t_gap	4 hour	Same (+0.0 %)	50,073 (-20.9 %)
t_gap	None	Same (+0.0 %)	50,007 (-21.0 %)

ECA^a/ECA^h and longer durations. ECA^h are more affected because of higher spatial granularity of human trajectories. These effects on duration and the areas can be seen in Table 5.

The effects of changing the value of HDA_radius can be seen in Figure 10; a histogram showing the smallest value of HDA_radius required for each encounter.

Both $height^h$ and $height^a$ appear to have low sensitivity: $height^h$ changing by 0.4 meters (a significant amount in human height) does not affect the number of EE or EC. While $height^a$ is more sensitive than $height^h$, its influence on the results remains marginal. Increasing or decreasing $height^a$ by 20% had less than a 1% change in the total number of EC and under 3% change in EE.

We analyzed doy_shift values from 0 to 15; but present only 0, 1, 2, 3, and 14 in Table 6 as the pattern remains consistent. doy_shift affects only the encounter's count and computation time, by selecting trajectory pairs for comparison, and does not influence any EC characteristics. On average, each additional day of doy_shift increases encounters by 3,954, with roughly half the increase between $real$ encounters and $doy\_shift = 0$.

Applying temporal resampling or Douglas–Peucker filtering alone strongly affect results. Larger min_dist values remove more human points, lowering granularity and inflating HDA size and duration. This merges consecutive HDAs, producing false encounters before or after human passage. The effect is problematic as merging, and thus HDA duration, depend only on trajectory geometry without accounting for temporality. The temporal resampling reduces sensitivity to min_dist by preserving temporal granularity, even with a large min_dist. The Douglas–Peucker filter retains abrupt geometric changes, while resampling preserves temporal granularity.

To assess the influence of t_gap, five values were tested (Table 6). As t_gap is more sensitive at lower values, we used smaller step sizes between t_gap at minutes scale. The parameter shows low sensitivity when it is large enough to prevent splitting a single encounter due to brief line-of-sight interruptions, yet small enough to distinguish encounters occurring on separate trajectory legs. It does not affect the number of EE, as t_gap only governs how they are grouped into encounters.

The d_gap^a parameter removes PPA where the points are at a distance greater than 500 m which results in very large PPA. These PPAs can arise from various factors, such as recording gaps or the animal traveling quickly over a period of time. While these segments are not inherently false, they often lead to encounters that are too large and imprecise to provide meaningful local insights. This parameter does not have a significant effect on the overall numbers of EE and EC, although the EC that are prevented by this parameter have extremely large ECA^a and have a significant effect on spatial analysis. Similarly to the d_gap^a, d_gap^h has little effect on the overall numbers of EE and EC, though the encounters prevented by this parameter have extremely large ECA^h.

5.3 Comparison with ORTEGA

In this section, we compare our method with ORTEGA method (Su et al., 2024; Dodge et al., 2021). As we already mentioned, the primary difference between ORTEGA and our method is based on the rational of HDAs and PPAs. In particular, PPA is meant to account for incompleteness in a trajectory by estimating where the moving object could be in between GNSS points. The HDA is designed

to account for the area surrounding a moving object's known path where it could potentially impact wildlife.

Using PPA as a stand in for disturbance area does not work well as the size of PPA are linked to incompleteness and not the behavior of the animal. As the human data had relatively little incompleteness, the median minor axis of PPA using the default settings was 25 m; significantly lower than any disturbance estimate for chamois.

Increasing the maximum speed or introducing artificial incompleteness would increase the size of the PPA, but these methods distort the meaning of the PPA and do not relate to human or animal behavior.

For comparison, ORTEGA was run on the default settings on all trajectory pairs with an encounter; Table 7 shows the precent of pairs with a detected encounter by distance. This indicates that the use of PPAs alone does not work well for encounters where the incompleteness is less significant than the distance that the objects affect each other. For instance, ORTEGA is not able to detect the encounters shown in Figure 6 as the PPA of the human trajectory are too small to intersect the animal PPAs. Only the presence or lack of detected encounter between trajectories pairs are compared between our method and ORTEGA as they do not use the same procedure for separating encounters.

Table 7. Encounters detected by ORTEGA

Min Encounter Distance	0-25m	25-50m	50-75m
Percent of detected EC	33%	14%	6%

5.4 Typical Analytical Approaches to Explore Encounters

In this section, we present two typical analytical approaches of how encounters can be analyzed by the potential users.

5.4.1 Seasonal Analysis

This section analyzes temporal encounter patterns using time of day and the season definitions from section 4.4. Table 8 shows the number of trajectories by season.

Table 8. Trajectory Count by Season

Moving object	Spring	Summer	Fall	Winter
Human	647	1042	597	551
Chamois	4351	4641	6344	3836

A histogram of when encounters took place during each season is depicted in Figure 11. The bin size for the histogram was set to 15 minutes, and encounters were assigned to all bins that overlapped with their duration, meaning a single encounter could be included in multiple bins.

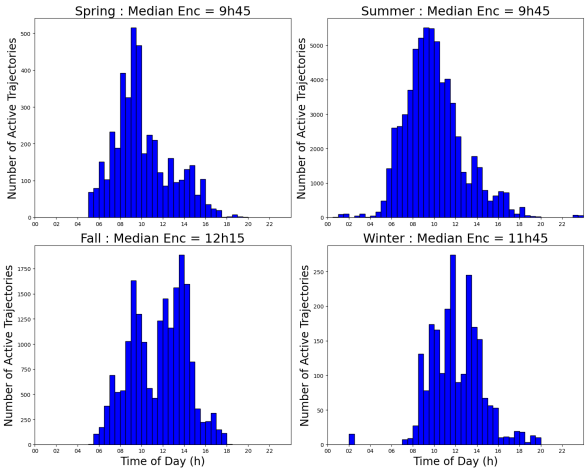

Figure 11. Histogram depicting the number of encounters that have a duration that intersects with each bin. Note that Y axis scales do not match for all seasons. Time in coordinated universal time (utc).

The greatest number of encounters took place during the summer, followed by the fall. The histogram reveals a bimodal distribution of encounters particularly during fall and winter. Two distinct peaks appear in these seasons: in the morning and in the early afternoon. This bimodal pattern is characteristic of typical human mobility behavior and closely reflect the same shape of the chamois activity pattern shown in (Thel et al., 2024).

We applied a kernel density estimation to compare the timing of encounters with the distribution of human trajectories. The same temporal resolution and constraints from Figure 11 were used, with each kernel centered on the middle of each time bin. The smoothing parameters for the kernel density were minimized while removing local peaks at each bin centers (0.1 for human trajectories and 0.2 for encounters) to maintain overall trends. Figure 12 displays the smoothed densities of encounters and human

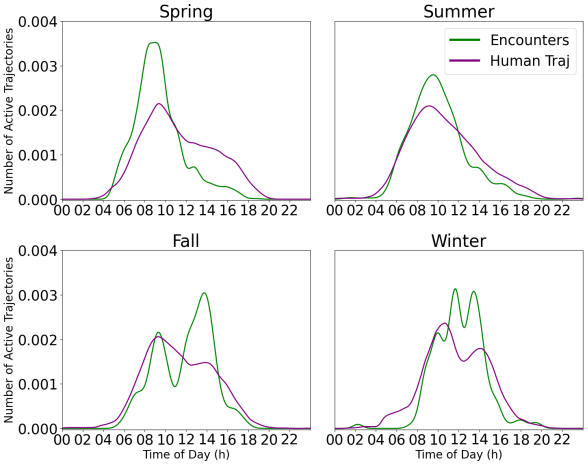

Figure 12. Kernel density estimate of human trajectories and encounters over season time (utc).

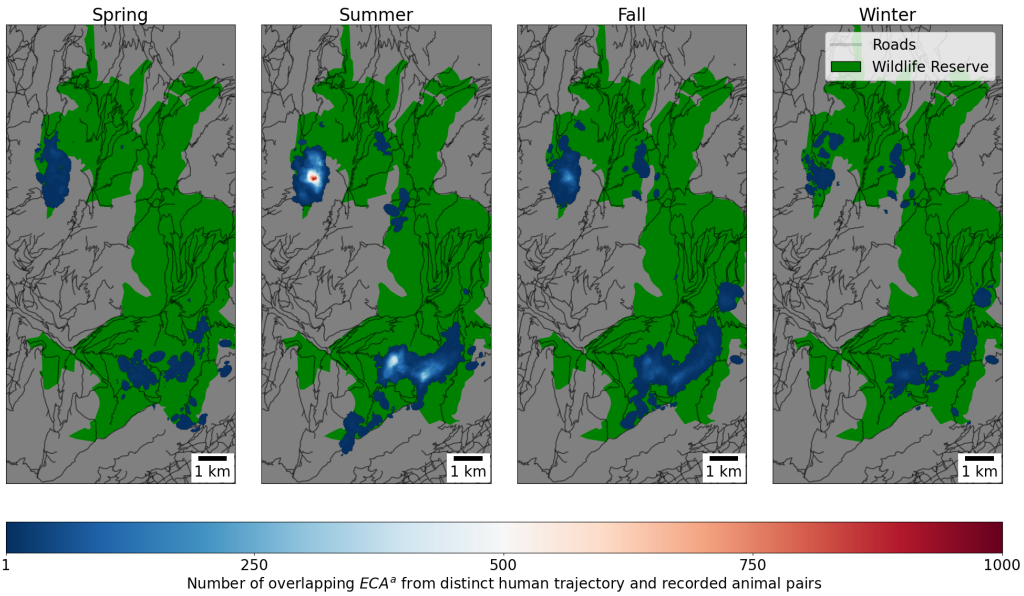

Figure 13. Heatmap of the number of $\boldsymbol{ECA^a}$ from unique human trajectory and individual chamois pairs.

trajectories across time. The results show that, in most seasons, higher numbers of human trajectories correspond with more encounters. However, in the fall, the second peak in encounters appears significantly higher than the corresponding peak in the number of human trajectories, suggesting a seasonal shift or a change in encounter dynamics during this season. This season corresponds to the rutting period during which males show increased activity and ranging behaviour associated with mate searching (Corlatti et al., 2013).

To visualize the spatial distribution of encounters over time, we used a heat map (see Figure 13). This approach allows for an intuitive and continuous representation of encounter density across space, making it easier to identify hot-spots. The map counts the number of unique pairs of human trajectory and individual animal by merging all ECA^a per pair prior to counting the number of merged ECA^a intersecting each cell. This avoids over representation of repeated encounters involving the same pair on different doy_shifts, while still capturing the full affected areas.

We can observe that in both summer and fall, encounters are widespread in both the northern and southern regions. In contrast, the winter season shows a higher proportion of encounters concentrated in the southern area, while the spring season shows the opposite trend, with more encounters in the northern area.

5.4.2 Atypical Encounter Analysis

This section deeply explores a set of encounters that deviates from the typical patterns, specifically, several encounters took place before 4:00 a.m. during the summer, as shown in Figure 11. These encounters are associated with three human trajectories.

All three trajectories, that we note here as A, B, and C, encountered multiple different chamois. Some chamois remained in the area, leading to multiple potential encounters at different doy_shifts, with the same animal. For example, trajectory A involved 53 encounters with 9 individual chamois. Notably, one chamois encountered all three people.

Trajectories A, and B represent runners. These are part of a larger set of trajectories associated with the same two persons. For example, person A has 71 recorded trajectories. Both persons have a mix of running and skiing trajectories, with encounters present in both activity types.

This type of analysis highlights the potential to explore encounter results across multiple dimensions such as repeated interactions with the same individuals, temporal distribution of activities, frequency of user presence, and activity types.

6 Conclusion and Future Work

This paper presents a novel method for detecting and spatializing human-wildlife encounters by integrating the concept of human disturbance area. The human disturbance area captures the spatial extent of human disturbance and potential encounters which accounts for limited representativeness of recorded trajectories. The method was implemented and tested using a large dataset of moving objects in the French Alps. A detailed analysis of sensitivity was made. Results showed that introducing intervisibility is necessary in a mountain context. Among the parameters considered, the HDA_radius has the most significant influence on the results, while other parameters have a comparatively minor effect, highlighting the robustness and reliability of the proposal.

This method provides a foundation for developing dynamic tools that allow stakeholders to explore, analyze, and visualize the impacts of human recreational activities in natural environments. To illustrate its relevance, we provided a set of typical user analysis tasks that demonstrate the benefits to stakeholders.

Several enhancements to the detection method are proposed. First, the current intervisibility computation, based on line-of-sight analysis, could be enhanced by adopting line-to-area or area-to-area visibility analysis in order to improve accuracy and enable consideration of varying degrees of intervisibility (e.g. complete or partial intervisibility).

Secondly, to assist decision-makers in managing human-wildlife disturbance, it is important to understand the context of the encounter as a more intricate function for determining HDA_radius could be implemented. As HDA_radius represents the disturbance of a person on wildlife, it should be able to account for contextual features such as environment (chamois feel protected in areas of steep slope (von Elsner-Schack, 1985)) as well as animal and human behaviors. As some human behavior can be more disruptive than others (Stankowich, 2008; Hamr, 1988; Taylor and Knight, 2003), in future work, we intend to semantically enhance both animal and human trajectories. For animals, this includes the annotation of behaviors such as resting, foraging, and traveling. For human trajectories, semantic enhancements will involve detecting stops and identifying between different modes of movement such as skiing or hiking.

Further validation will integrate in-situ data, the low granular data not analyzed in this work, insights from ecological studies, and collaboration with stakeholders. As the method has been tested with medium granularity of data, the unused data will be reincorporated and tested to determine its effect. To address representativeness of recorded data, we aim to train a machine learning model on the spatial and temporal context of encounters to be able to extrapolate the most likely areas to have encounters to try and capture encounter zones in areas with less data.

Finally, this method was applied to two types of moving objects: humans and chamois in a mountainous area. Nevertheless, we claim that, due to its generality, it can be easily adapted to other animals or moving objects, as well as to different environments.

Declaration of Generative AI in Writing

The authors declare that they have used Generative AI tools in the preparation of this manuscript. Specifically, the AI tools were utilized for improving grammar, and sentence structure, but not for generating scientific content, research data, or substantive conclusions. All intellectual and creative work, including the analysis and interpretation of data, is original and has been conducted by the authors without AI assistance.

Acknowledgements

This work was supported by the ANR under grant agreement no. ANR-23-CE55-0003 (IntForOut research Project: Multisource spatial data INTegration FOR the Monitoring of Ecosystems under the pressure of OUTdoor recreation). We warmly thank all professionals, colleagues, and volunteers for their contributions to chamois capture and marking, the recovery of GPS collars, and their involvement in the management and collection of GPS data on both animal movements and human activities (OFB, LECA, GIC, PNR des Bauges, ONF, and Edytem). Thank you to Baptiste Morel for supplying Strava data used in this paper.

References

Balmford, A., Green, J. M., Anderson, M., Beresford, J., Huang, C., Naidoo, R., Walpole, M., and Manica, A.: Walk on the wild side: estimating the global magnitude of visits to protected areas, PLoS biology, 2015.

Bjørneraas, K., Van Moorter, B., Rolandsen, C. M., and Herfindal, I.: Screening Global Positioning System Location Data for Errors Using Animal Movement Characteristics, J Wildl Manag, 2010.

Bogorny, V., Renso, C., de Aquino, A. R., de Lucca Siqueira, F., and Alvares, L. O.: CONSTAnT – A Conceptual Data Model for Semantic Trajectories of Moving Objects, Transactions in GIS, 18, https://doi.org/10.1111/tgis.12011, 2014.

Boukhers, Z., Wang, Y., Shirahama, K., Uehara, K., and Grzegorzek, M.: Convoy detection in crowded surveillance videos, in: Human Behavior Understanding: 7th International Workshop, HBU 2016, Amsterdam, The Netherlands, October 16, 2016, Proceedings 7, Springer, 2016.

Corlatti, L., Caroli, M., Pietrocini, V., and Lovari, S.: Rutting Behaviour of Territorial and Nonterritorial Male Chamois: Is There a Home Advantage?, Behavioural processes, 92, 118–124, 2013.

Courbin, N., Garel, M., Marchand, P., Duparc, A., Debeffe, L., Börger, L., and Loison, A.: Interacting lethal and nonlethal human activities shape complex risk tolerance behaviors in a mountain herbivore, Ecological Applications, 32, https://doi.org/10.1002/eap.2640, 2022.

Crampe, J.-P., Bon, R., Gerard, J.-F., Serrano, E., Caens, P., Florence, E., and Gonzales, G.: Site Fidelity, Migratory Behaviour, and Spatial Organization of Female Isards (*R*upicapra Pyrenaica) in the Pyrenees National Park, France, Canadian Journal of Zoology, 85, 16–25, 2007.

Darmon, G., Calenge, C., Loison, A., Jullien, J., Maillard, D., and Lopez, J.: Spatial distribution and habitat selection in coexisting species of mountain ungulates, Ecography, 35, https://doi.org/10.1111/j.1600-0587.2011.06664.x, 2012.

Daubal, M., Fajinmi, O., Jangaard, L., Simonson, N., Yasutake, B., Newell, J., and Ali, M.: Safe step: a real-time gps tracking and analysis system for criminal activities using ankle bracelets, in: Proceedings of the 21st ACM SIGSPATIAL International Conference on Advances in Geographic Information Systems, 2013.

Dodge, S., Su, R., Johnson, J., Simcharoen, A., Goulias, K., Smith, J. L. D., and Ahearn, S. C.: ORTEGA: An object-oriented time-geographic analytical approach to trace space-time contact patterns in movement data, Computers, Environment and Urban Systems, 88, https://doi.org/10.1016/j.compenvurbsys.2021.101630, 2021.

Doncaster, C. P.: Non-parametric estimates of interaction from radio-tracking data, Journal of Theoretical Biology, 143, https://doi.org/10.1016/S0022-5193(05)80020-7, 1990.

Douglas, D. H. and Peucker, T. K.: Algorithms for the reduction of the number of points required to represent a digitized line or its caricature, Cartographica: the international journal for geographic information and geovisualization, 10, 112–122, 1973.

Downs, J. A., Lamb, D., Hyzer, G., Loraamm, R., Smith, Z. J., and O'Neal, B. M.: Quantifying spatio-temporal interactions of animals using probabilistic space–time prisms, Applied Geography, 55, https://doi.org/10.1016/j.apgeog.2014.08.010, 2014.

Duparc, A., Garel, M., Marchand, P., Dubray, D., Maillard, D., and Loison, A.: Revisiting the functional response in habitat selection for large herbivores: a matter of spatial variation in resource distribution?, Behavioral Ecology, 30, 1725–1733, 2019.

Hamr, J.: Disturbance Behaviour of Chamois in an Alpine Tourist Area of Austria, Mountain Research and Development, 8, https://doi.org/10.2307/3673407, 1988.

Ho, K. and Loraamm, R.: Using a Cost-Distance Time-Geographic Approach to Identify Red Deer Habitat Use in Banff National Park, Alberta, Canada, ISPRS International Journal of Geo-Information, 12, https://doi.org/10.3390/ijgi12080339, 2023.

Huang, Y., Chen, L., Chen, P., Negenborn, R. R., and Van Gelder, P.: Ship collision avoidance methods: State-of-the-art, Safety science, 121, 451–473, 2020.

IGN: BD ALTI, https://geoservices.ign.fr/bdalti, 2025.

IGN: BD TOPO, https://geoservices.ign.fr/bdtopo, 2025.

Ivanovic, S.: Quality based approach for updating geographic authoritative datasets from crowdsourced GPS traces, PhD Thesis, Paris Est, 2018.

Kerouanton, C.: Eye catching vs Breath Catching, PhD Thesis, Université de Savoie, Chambéry, FRA., 2020.

Lonergan, C. and Hedley, N.: Unpacking isovists: a framework for 3D spatial visibility analysis, Cartography and Geographic Information Science, 43, 87–102, 2016.

Long, J.: Spatial Methods for Understanding Human-Wildlife Interactions, Spatial Knowledge and Information Canada, 2019.

Long, J. A., Webb, S. L., Nelson, T. A., and Gee, K. L.: Mapping areas of spatial-temporal overlap from wildlife tracking data, Mov Ecol, 3, https://doi.org/10.1186/s40462-015-0064-3, 2015.

Lührs, M. L. and Kappeler, P. M.: Simultaneous GPS tracking reveals male associations in a solitary carnivore, Behavioral Ecology and Sociobiology, 2013.

Marion, J., Leung, Y.-F., and Nepal, S.: Monitoring Trail Conditions: New Methodological Considerations, The George Wright forum, 23, 2006.

Méneroux, Y. and van Damme, M.-D.: Tracklib: a python library with a variety of tools, operators and functions to manipulate GPS trajectories, Ph.D. thesis, Laboratoire sciences et technologies de l'information géographique, 2024.

Meratnia, N. and de By, R. A.: Spatiotemporal compression techniques for moving point objects, in: Advances in Database Technology-EDBT 2004: 9th International Conference on Extending Database Technology, Heraklion, Crete, Greece, March 14-18, 2004 9, 2004.

Miller, J. A.: Towards a Better Understanding of Dynamic Interaction Metrics for Wildlife: a Null Model Approach, Transactions in GIS, 19, https://doi.org/10.1111/tgis.12149, 2015.

Ramer, U.: An iterative procedure for the polygonal approximation of plane curves, Computer graphics and image processing, 1, 244–256, 1972.

Spaccapietra, S., Parent, C., Damiani, M. L., de Macedo, J. A., Porto, F., and Vangenot, C.: A conceptual view on trajectories, Data & knowledge engineering, 65, 2008.

Stankowich, T.: Ungulate flight responses to human disturbance: A review and meta-analysis, Biological Conservation, 141, https://doi.org/10.1016/j.biocon.2008.06.026, 2008.

Su, R., Liu, Y., and Dodge, S.: ORTEGA v1.0: an open-source Python package for context-aware interaction analysis using movement data, Mov Ecol, 12, https://doi.org/10.1186/s40462-024-00460-2, 2024.

Taylor, A. R. and Knight, R. L.: Wildlife Responses to Recreation and Associated Visitor Perceptions, Ecological Applications, 13, https://doi.org/10.1890/1051-0761(2003)13[951:WRTRAA]2.0.CO;2, 2003.

Thel, L., Garel, M., Marchand, P., Bourgoin, G., and Loison, A.: Too hot or too disturbed? Temperatures more than hikers affect circadian activity of females in northern chamois, Animal Behaviour, 210, https://doi.org/10.1016/j.anbehav.2024.01.010, 2024.

von Elsner-Schack, I.: What is good chamois habitat, The biology and management of mountain ungulates, pp. 71–76, 1985.

Yin, Z.-C., Liu, H., Zhang, Z.-J., Jin, Z.-H.-N., Li, S.-J., and Xiao, J.-Q.: Probabilistic Model of Random Encounter in Obstacle Space, ISPRS International Journal of Geo-Information, 8, https://doi.org/10.3390/ijgi8010032, 2019.

Ólafsdóttir, R. and Runnström, M. C.: Assessing hiking trails condition in two popular tourist destinations in the Icelandic highlands, Journal of Outdoor Recreation and Tourism, 3, 2013.

Čučković, Z.: Visibility Analysis, version 1.9.2, 2025.